Iranian Journal of Medical Physics
Vol. 12, No. 4, Autumn 2015, 262-270
Received: August 15, 2015; Accepted: March 12, 2016

Original Article

Experimental Evaluation of Depth Dose by Exit Surface Diode Dosimeters for Off-Axis Wedged Fields in Radiation Therapy

Alireza Mohammadkarim[1,2], Hasan Ali Nedaie[3*], Mahmoud Allahverdi[4], Mahbod Esfehani[5], Alireza Shirazi[6], Ghazale Geraily[6]

Abstract

Introduction
Evaluation of the delivered dose of externally wedged photon beams by external diode dosimeters during the treatment process requires the estimation of exit surface dose correction factors in various wedge angles and field sizes.
Materials and Methods
A system of absorbed dose evaluation, using p-type diode dosimeters placed on the exit surface of a phantom, was characterized for externally wedged photons with the maximum square field size. The values of wedge correction factor on the exit surface of the polystyrene phantom were determined for ^{60}Co and 6 MV photons. Then, the wedge correction factors were estimated at desirable depths.
Results
Based on the findings, the deviation of off-axis wedge correction factors of the exit surface wedged fields from the central axis factor may be as large as ±10% at the evaluated depths. The results showed that the absorbed dose at each depth of patient tissue could be estimated by applying an accurate exit wedge correction factor for that particular depth, with negligible probable errors (below 1.5%).
Conclusion
In case positioning a diode dosimeter on the patient's entrance surface of a phantom of patients is troublesome, the diode dosimeter can be placed on the exit surface in order to evaluate the absorbed dose for externally wedged photons. Based on the findings, exit dose correction factors for wedged beams cannot be discarded; in fact, these factors are variable at different directions of externally wedged beams.

Keywords: Absorbed Dose, Diode Dosimeter, Wedge, Field Size, Radiation Therapy

1- Department of Medical Radiation Engineering, Science and Research Branch, Islamic Azad University, Tehran, Iran
2- Ph.D student, Department of Medical Physics, Faculty of Medical Sciences, Tarbiat Modares University, Tehran, Iran
3- Department of Radiotherapy, Oncology and Medical Physics, Tehran University of Medical Sciences, Tehran, Iran
*Corresponding author: +98 21 66948673, Fax: +98 21 66581638, E-mail: Nedaieha@sina.tums.ac.ir

4- Department of Medical Physics, Tehran University of Medical Sciences, Tehran, Iran
5- Department of Radiation Oncology, Cancer Institute of Iran, Tehran University of Medical Sciences, Tehran, Iran
6- Department of Medical Physics, Tehran University of Medical Sciences, Tehran, Iran

1. Introduction

As recommended by the International Commission of Radiological Units and Measurements (ICRU), the delivered dose to a tumor should fall within ±5% of the prescribed dose [1]. In vivo dosimetry, as the only tool for evaluating the actual delivered dose to the patient, is recommended for the quality improvement of patient care in radiation therapy. Overall, n vivo dosimetry programs have been shown to be highly effective in detecting various types of errors in the dose delivery process [2-4].

In vivo diode dosimetry is a reliable method for patient dose control. The major advantage of diodes, compared to other dosimeters such as film and thermoluminescent dosimeters, is their instant readout after radiation [5-8]. It should be noticed that a set of correction factors is required to account for the variations in diode response in positions deviating from the reference conditions [1-3, 7-12].

Unlike open beams, while using wedged photon beams at various positions of wedged and non-wedged direction s, off-axis diode correction factors differ from those at the central point [12, 13]. Variations in off-axis wedge correction factors for entrance surface diodes have been reported in previous studies [5, 12], and coordinated measurements of entrance and exit doses have been performed, using diode dosimeters in order to calculate the delivered dose of externally wedged beams [13]. However, the influence of externally wedged beams on diode readings of the exit surface has not been investigated, so far.

Such investigations are of great significance, since in clinical measurements where the entrance surface is situated on the device couch (i.e., the angle between the gantry and couch is about 270), it is impossible to place the dosimeter on the entrance surface. Moreover, the geometric shape of some organs restrains diode implementation on the entrance surface. Therefore, development of a new method, based on exit dosimeter measurements, is essential for estimating the target dose in externally wedged beams.

In this study, we aimed to estimate the wedge correction factors in different modes, i.e., off-axis wedged (thin and thick edges of the wedge) and non-wedged direction s, on the exit surface of a polystyrene phantom. In this research, we aimed to present a systematic study on the influence of exit wedge correction factors at external positions on the absorbed dose for two ranges of photon beams and suggest a viable procedure for estimating the absorbed dose.

It should be mentioned that the purpose of the current study was not to introduce a novel algorithm to compete with or question the available methods at different wedged beam positions, but to investigate whether exit surface diode measurements could be regarded as a reliable method for dose verification of externally wedged photons.

2. Materials and Methods

All measurements were performed, using T60010L (a p-type diode for 1-5MV photon beams) and T60010M (a p-type diode for 5-13MV photon beams) dosimeters (PTW, Freiburg, Germany). Calibration was achieved with the diodes positioned on the exit surface of a polystyrene phantom with a thickness of 15 cm for a 10×10 cm^2 field, using the reference source-skin distance (SSD)i.e., 80 cm for ^{60}Co and 100 cm for 6 MV photon beams.

Before the routine use of diodes, signal stability test was performed, as described in previous research [14, 15]. As the diodes could show various sensitivities to temperature and direction correction factors, which were appropriate for temperature and the angle between the symmetric axis of diode and beam axis, were applied in each reading, using a method proposed in a previous study [14].

For ^{60}Co and 6 MV irradiations, 780C ^{60}Co machine (Theratronics, Ontario, Canada) and Varian Clinac 2100C (Varian Medical Systems, Palo Alto, CA, USA) were employed, respectively. In order to estimate the exit wedge correction factor at each depth, the diode dosimeter was placed on the exit surface of the polystyrene phantom.

Afterwards, calibration was performed for each diode, positioned on the exit surface of the phantom at the central beam axis (10×10 cm^2 field) against an ionization chamber system at reference SSD.

A TM31013 Farmer chamber (0.3 cm^3) and a TM30010 Farmer chamber (0.6 cm^3), produced by PTW Freiburg (Germany),were used as the reference dosimeters for ^{60}Co and 6 MV photon beams, respectively. The exit dose calibration factor ($F_{cal,ex}$) was determined as the ratio of the absorbed dose, measured by the ionization chamber (D) at the build-down depth ($d_{m,ex}$) to the semiconductor signal reading (R) on the exit surface with a build-up layer under reference conditions [3, 6, 13].

According to previous studies on exit dose correction factors, the exit field size correction factor (CF_{ex}) for a non-standard field size (a×a) was defined as follows:

$$CF_{ex} = \left[(D/R)_{[a\times a]} / (D/R)_{[10\times 10]}\right]_{ex} \quad (1)$$

Moreover, the exit wedge correction factor ($CF_{w,ex}$) with a non-reference field size was estimated as follows:

$$CF_{w,ex} = \left[\begin{matrix}(D_{[wedgedbeam,a\times a]} / R_{[openbeam,a\times a]}) \div \\ (D_{[wedgedbeam,10\times 10]} / R_{[openbeam,10\times 10]})\end{matrix}\right]_{ex} \quad (2)$$

For this purpose, the gantry angle needed to be set at 180º (Figure 1).

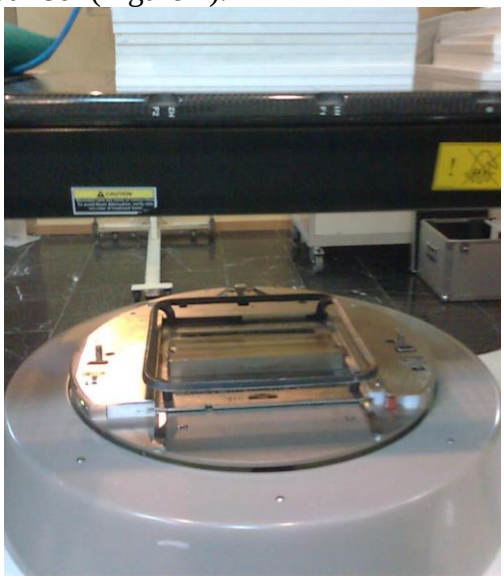

Figure 1. The angle between the central beam axis and the symmetry axis of the diode regulated about 180º for $CF_{w,ex}$ measurement

Then, diode dosimeters and ionization chambers were required to be shifted from the central beam axis at the specified distance. The method of using diodes, ionization chamber, and schematic diode positions, relative to central axis for wedged fields, are presented in figures 2, 3, and 4, respectively.

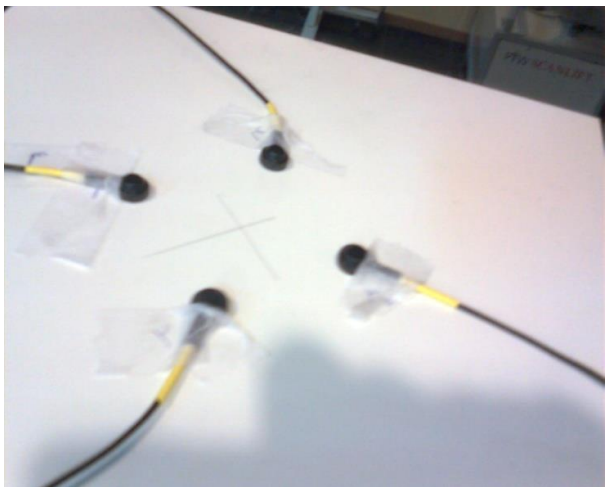

Figure 2. Method of diode displacement out of the central beam axis

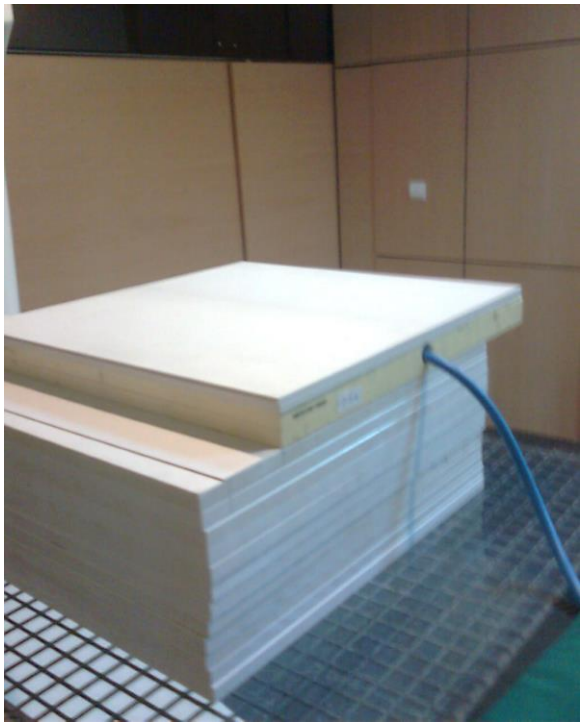

Figure 3. Displacement of the ionization chamber out of the central beam axis by shift by the slab where the

ionization chamber is located

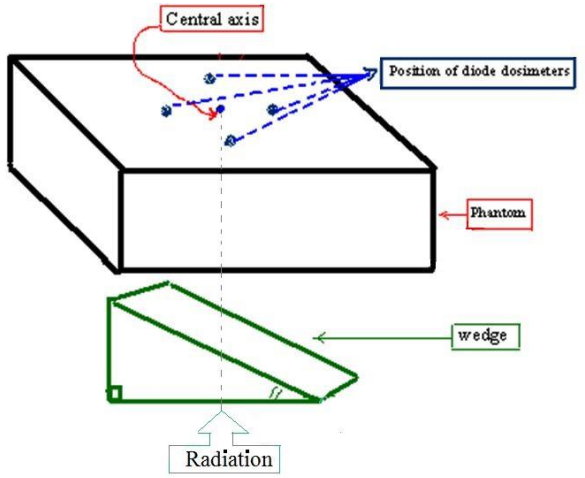

Figure 4. The schematic figure showing diode dosimeter positions relative to the central beam axis in wedged fields

The exit depth transmission ($T_{d,ex}$) was determined as the ratio of the absorbed dose, measured with the Farmer ionization chamber at each depth (D_d) to the absorbed dose, calculated with the Farmer ionization chamber at the build-down depth ($D_{m,ex}$) on the exit surface of the phantom [13]:

$$T_{d,ex} = \frac{D_d}{D_{m,ex}} = \frac{D_d / D_{m,en}}{D_{m,ex} / D_{m,en}} = \frac{(Percentage\ Depth\ Dose)_d}{(Percentage\ Depth\ Dose)_{ex}} = \frac{PDD_d}{PDD_{ex}} \quad (3)$$

Where $D_{m,en}$ is the absorbed dose at the build-up depth.

The exit dose was not measured under complete photon backscatter conditions. Therefore, the backscatter correction factor (BSF) was determined as the ratio of the Farmer ionization chamber reading under full backscatter conditions (R_{FB}) to the reading under exit dose measurement conditions (R_{MC}) for different field sizes [3, 13]:

$$BSF = \frac{R_{FB}}{R_{MC}} \quad (4)$$

The correction factors for various physical parameters, i.e., field size, SSD, thickness, temperature, gantry angle, and dose rate, should be applied in diode reading at each step, as mentioned in previous studies [5, 13, 14, 16, 17]. Then, the expected wedge correction factors at each depth ($CF_{w,d}$) were used, since the measurements were carried out inactual situations out of the central axis [13, 18]. $CF_{w,d}$ was determined, using the following formula:

$$CF_{w,d} = CF_{w,ex} \times T_{d,ex} \times BSF \quad (5)$$

In th repeated is study, all diode and ionization chamber measurements were repeated four times, and the average value was used for accurate calculations In clinical application, the estimated dose to the target (D_{target}) was deduced from diode reading (R_r) by applying a proper calibration factor (F_{cal}), which was corrected by $CF_{w,d}$ [5, 12, 13].

To analyze the accuracy of dose estimations in this study, the calculated doses were acquired from exit surface diode readings at different externally wedged beam points after applying the correction factors. Then, the absorbed dose at each depth was directly measured with the ionization chamber and compared with the calculated values.

3. Results

$CF_{w,ex}$ values were determined for each beam quality. First, the data related to various wedged fields of ^{60}Co photons were obtained for the maximum square field size. Table 1 shows the estimated $CF_{w,ex}$ as a function of off-axis distance for30^o, 45 ^{o}, and 60 ^{o} wedges at a field size of 10×10 cm^2 for ^{60}Co photon beams. In this table, the data are related to two different positions, i.e., the wedged direction "x" (positive or negative signs of “x“ indicate the off-axis position towards the thick or thin edges, respectively) and non-wedged direction "y".

Afterwards, $CF_{w,ex}$ was determined for 15^o, 30^o, 45^o, and 60^o wedged fields for 6 MV photon beams at the maximum achievable square field size with wedges (15×15 cm^2) and the reference field size (10×10 cm^2). In tables 2(a) and 2(b) , the estimated $CF_{w,ex}$ values are shown as a function of off-axis distance in wedged and non-wedged directions at the mentioned field sizes for 6 MV photon beams.

As presented in Table 1, maximum $CF_{w,ex}$ variations for ^{60}Co photons in wedged and non-wedged directions were 8% and 4%, respectively for a field size of 10×10 cm^2. Also, the data in tables 2(a) and 2(b) show that

maximum $CF_{w,ex}$ variations for 6 MV photons in wedged and non-wedged directions were 5.6% and 1% for the 10×10 cm^2 field size and 6.8% and 2% for the 15×15 cm^2 field size, respectively.

Table 3 indicates the exit correction factor s, calculated by equation 1, for various open field sizes ($CF_{f.s,ex}$) of ^{60}Co and 6 MV beams. As demonstrated in this table, $CF_{f.s,ex}$ for ^{60}Co photons decreased by nearly 6.3% when the field size increased from 5×5 cm^2 to 20×20 cm^2. However, $CF_{f.s,ex}$ for 6 MV photons increased by approximately 2.2% as the field size increased from 5×5 cm^2 to 20×20 cm^2.

In Table 4, the effect of BSF is plotted as a function of the collimator opening for ^{60}Co and 6 MV photon beams. According to this table, BSF variations for ^{60}Co photons were larger than those for 6 MV photons, as the field size increased from 5×5 cm^2 to 20×20 cm^2. The $T_{d,ex}$ for ^{60}Co photon beams in a field size of 10×10 cm^2 and $CF_{d,ex}$ for 6 MV photon beams in a field size of 15×15 cm^2under reference conditions are presented in Table 5 at build-up ($d_{m,en}$), 5 cm, 10 cm, and build-down depths ($d_{m,ex}$).

As reported in previous investigations, PDD_d values of wedged fields in all directions at any desirable off-axis distance are approximately equal to those of open fields at the central beam axis [12, 13, 19, 20]. Therefore, in the present study, PDD_d values of open fields at the central beam axis were used for calculations, as applied in equation 3.

Table 1. Variations of $CF_{w,ex}$ values for ^{60}Co photons at a 10×10 cm^2 field size in wedged (x) and non-wedged (y) directions for three different wedges under reference conditions

Wedge angle	Off-axis distance in wedged direction "x" (cm)							Off-axis distance in non-wedged direction "y" (cm)			
	-4	-3	-2	0	2	3	4	0	±2	±3	±4
30º	0.951	0.959	0.960	0.977	0.981	0.983	0.988	0.977	0.966	0.963	0.939
45º	0.938	0.945	0.947	0.956	0.971	0.982	0.985	0.956	0.925	0.924	0.923
60º	0.912	0.913	0.921	0.934	0.966	0.989	0.994	0.934	0.913	0.908	0.901

Table 2. Variations of$CF_{w,ex}$ values for 6 MV photons in wedged (*x*) and non-wedged (*y*) directions for four different wedges under reference conditions.

(a) For the 15×15 cm^2 field size

Wedge angle	Off-axis distance in wedged direction "x" (cm)							Off-axis distance in non-wedged direction "y" (cm)			
	-6	-4	-2	0	2	4	6	0	±2	±4	±6
15º	1.044	1.039	1.033	1.024	1.023	1.020	1.020	1.024	1.018	1.018	1.017
30º	1.040	1.033	1.026	1.016	1.011	1.004	1.003	1.016	1.013	1.013	1.012
45º	1.039	1.034	1.022	1.016	1.004	0.996	0.994	1.016	1.011	1.011	1.007
60º	1.048	1.039	1.026	1.022	0.997	0.986	0.980	1.022	1.017	1.016	1.005

(b) For the 10×10 cm^2 field size

Wedge angle	Off-axis distance in wedged direction "x" (cm)					Off-axis distance in non-wedged direction "y" (cm)		
	-4	-2	0	2	4	0	±2	±4
15º	1.033	1.026	1.017	1.016	1.014	1.017	1.012	1.010
30º	1.027	1.020	1.009	1.005	0.998	1.009	1.007	1.006
45º	1.028	1.017	1.009	0.999	0.990	1.009	1.005	1.005
60º	1.035	1.021	1.016	0.991	0.980	1.016	1.011	1.009

Table 3. $CF_{f.s,ex}$ as a function of square field size for ^{60}Co and 6 MV photon beams under reference conditions

Photon energy	Field size (cm)						
	5	8	10	12	15	18	20
^{60}Co	1.052	1.022	1.000	1.000	1.000	0.992	0.988
6 MV	0.988	0.995	1.000	1.004	1.005	1.009	1.010

Table 4. BSF as a function of square field size for ^{60}Co and 6 MV photon beams under reference conditions

Photon energy	Field size (cm)						
	5	8	10	12	15	18	20
^{60}Co	1.022	1.030	1.040	1.052	1.064	1.068	1.070
6MV	1.003	1.007	1.011	1.013	1.018	1.023	1.026

Table 5. $T_{d,ex}$ with maximum possible square field for ^{60}Co and 6 MV photon beams at different depths of 15 cm phantom

Photon energy	Field size (cm^2)	SSD (cm)	Depth (cm)			
			$d_{m,en}$	5	10	$d_{m,ex}$
^{60}Co	10×10	80	2.550	2.009	1.436	1.000
6 MV	15×15	100	1.766	1.549	1.222	1.000

Table 6. $CF_{w,d}$ in wedged (x) and non-wedged (y) directions for different wedges, employing a ^{60}Co beam between the entrance and exit depths

Wedge angle	Depth (cm)	Off-axis distance in wedged direction "x" (cm)							Off-axis distance in non-wedged direction "y" (cm)			
		-4	-3	-2	0	2	3	4	0	±2	±3	±4
30°	0.5	2.522	2.543	2.546	2.591	2.602	2.607	2.620	2.591	2.562	2.554	2.490
	5	1.987	2.004	2.006	2.041	2.050	2.054	2.064	2.041	2.018	2.012	1.962
	10	1.422	1.434	1.436	1.461	1.467	1.470	1.478	1.461	1.445	1.440	1.404
	14.5	0.989	0.997	0.998	1.016	1.020	1.022	1.027	1.016	1.005	1.002	0.977
45°	0.5	2.488	2.506	2.511	2.535	2.575	2.604	2.612	2.535	2.453	2.450	2.448
	5	1.960	1.974	1.979	1.997	2.029	2.052	2.058	1.997	1.933	1.931	1.928
	10	1.402	1.413	1.416	1.430	1.452	1.469	1.473	1.430	1.383	1.382	1.380
	14.5	0.976	0.983	0.985	0.994	1.010	1.021	1.024	0.994	0.962	0.961	0.960
60°	0.5	2.418	2.421	2.442	2.477	2.561	2.623	2.636	2.477	2.421	2.408	2.389
	5	1.905	1.908	1.924	1.951	2.018	2.066	2.077	1.951	1.908	1.897	1.883
	10	1.364	1.365	1.377	1.397	1.445	1.479	1.487	1.397	1.365	1.358	1.347
	14.5	0.949	0.950	0.958	0.973	1.005	1.029	1.034	0.973	0.950	0.944	0.937

Table 7. $CF_{w,d}$ in wedged(x) and non-wedged(y) directions for different wedges, employing a 6 MV beam between the entrance and exit depths

Wedge angle	Depth (cm)	Off-axis distance in wedged direction "x" (cm)							Off-axis distance in non-wedged direction "y" (cm)			
		-6	-4	-2	0	2	4	6	0	±2	± 4	±6
15°	1.6	1.877	1.868	1.857	1.841	1.839	1.834	1.834	1.841	1.830	1.830	1.828
	5	1.646	1.638	1.629	1.615	1.613	1.608	1.608	1.615	1.605	1.605	1.604
	10	1.299	1.293	1.285	1.274	1.273	1.269	1.269	1.274	1.266	1.266	1.265
	13.4	1.063	1.058	1.052	1.042	1.041	1.038	1.038	1.042	1.036	1.036	1.035
30°	1.6	1.870	1.857	1.845	1.827	1.818	1.805	1.803	1.827	1.821	1.821	1.819
	5	1.640	1.629	1.618	1.602	1.594	1.583	1.582	1.602	1.597	1.597	1.596
	10	1.294	1.285	1.276	1.264	1.258	1.249	1.248	1.264	1.260	1.260	1.259
	13.4	1.059	1.052	1.044	1.034	1.029	1.022	1.021	1.034	1.031	1.031	1.030
45°	1.6	1.868	1.859	1.837	1.827	1.805	1.791	1.787	1.827	1.818	1.818	1.810
	5	1.638	1.630	1.612	1.602	1.583	1.571	1.567	1.602	1.594	1.594	1.588
	10	1.295	1.286	1.271	1.264	1.249	1.239	1.237	1.264	1.258	1.258	1.252
	13.4	1.058	1.053	1.040	1.034	1.022	1.014	1.012	1.034	1.029	1.029	1.025
60°	1.6	1.884	1.868	1.845	1.837	1.792	1.773	1.762	1.837	1.828	1.827	1.807
	5	1.653	1.638	1.618	1.616	1.572	1.555	1.545	1.616	1.604	1.602	1.585
	10	1.304	1.293	1.276	1.271	1.240	1.227	1.219	1.271	1.265	1.263	1.250
	13.4	1.067	1.058	1.044	1.040	1.015	1.004	0.998	1.040	1.035	1.034	1.023

Table 8. Comparison of the calculated and measured dose s out of the central beam axis in the wedged direction (towards the thick edge [+x] and towards the thin edge [-x] of the wedge) and non-wedged direction (±y)

(a) At three positions for a ^{60}Co photon beam in a 10×10 cm^2 filed with 30°, 45°, and 60° wedgesTarget dose value (cGy)

	Pos. 1: Wedge angle=30°, d=5 cm, off-axis distance=3 cm			Pos. 2: Wedge angle=45°, d=10 cm, off-axis distance=2 cm			Pos. 3: Wedge angle=60°, d=0.5 cm, off-axis distance=4 cm		
	x=-3 cm	x=+3 cm	y=±3 cm	x=-2 cm	x=+2 cm	y=±2 cm	x=-4 cm	x=+4 cm	y=±4 cm
Meas.	40.95	29.52	32.69	23.68	17.30	18.16	46.96	13.62	20.89
Cal.	41.00	29.27	32.31	24.02	17.18	18.18	47.61	13.80	21.18

(b) At four positions for the 15×15 cm^2 field of a 6 MV photon beam with 15°, 30°, 45°, and 60° wedges

Target dose value (cGy)

	Pos. 1: Wedge angle=15°, d=13.4 cm, off-axis distance=2 cm			Pos. 2: Wedge angle=30°, d=5 cm, off-axis distance=4 cm			Pos. 3: Wedge angle=45°, d=10 cm, off-axis distance=6 cm			Pos. 4: Wedge angle=45°, d=10 cm, off-axis distance=4 cm		
	x=-2cm	x=+2 cm	y=±2 cm	x=-4 cm	x=+4 cm	y=±4 cm	x=-6 cm	x=+6 cm	y=±6 cm	x=-4 cm	x=-4 cm	x=-4 cm
Meas.	48.09	45.85	46.99	65.04	51.66	58.34	46.65	26.53	34.79	41.01	22.27	30.12
Cal.	48.39	46.45	47.26	65.77	51.99	58.70	47.04	26.14	34.74	41.10	23.17	30.22

The $CF_{w,d}$ values were obtained, using equation 5 at each position. Table 6 shows $CF_{w,d}$ variations for ^{60}Co beams in all three wedge angles at a 10×10 cm^2 field in "x" and "y" directions at depths of 5 cm, 10 cm, $d_{m,en}$ (0.5 cm), and $d_{m,ex}$ (14.5 cm). Also, Table 7 presents the variations of $CF_{w,d}$by using a 6 MV photon beam for all four wedge angles at a 15×15 cm^2 field in "x" and "y" directions at depths of 5 cm, 10 cm, $d_{m,en}$ (1.6 cm), and $d_{m,ex}$ (13.4 cm).

The measured and calculated dose s by the use of ^{60}Co photon beams for the mentioned wedge angles at three typical positions are presented in Table 8(a). Moreover, comparison of measurements and calculations for 6 MV

photon beams are presented in Table 8(b). Based on these findings, maximum differences between the measured and calculated doses for different beam qualities were within ±1.5% at all exit surface diode measurements (not presented here).

4. Discussion

Comparison of data presented in tables 1 and 2 shows that maximum $CF_{w,ex}$ variations for a 10×10 cm^2 field in wedged and non-wedged directions were larger for ^{60}Co photon beams than 6 MV photon beams. This can be attributed to greater beam scattering for ^{60}Co photons, relative to 6 MV photons.

Based on the comparison of data presented in tables 2(a) and 2 (b) and the exit field size correction factor at the 15×15 cm^2 field (about 1.005) for 6 MV photons (Table 3), it can be deduced that an off-axis correction factor at a non-reference field size (a×a) could be approximated by multiplying the given correction factor at a reference field size (10×10) and the correction factor for the corresponding field size:

$$CF_{w,ex}\ (a\times a)= CF_{f.s,ex}\times CF_{w,ex}\ (10\times 10) \quad (6)$$

The results of the present study show that the exit field size correction factor is required to account for the difference in diode response s between the reference and non-reference wedged fields. Previous studies have reported similar findings for entrance diode measurements [2, 5, 12].

Based on the results presented in tables 6 and 7, with similar beam qualities and physical conditions, change of wedge angle, without applying the related correction factors, may exert significant effect s on the absorbed dose calculations. For instance, $CF_{d,ex}$ for ^{60}Co beam in a 10×10 cm^2 fieldwith a 3 cm off-axis distance in the non-wedged direction (y= $\pm$3 cm) would be 1.440 and 1.358 for 30^o and 60^o wedged photon beams at a depth of 10 cm, respectively. Similarly, the corresponding values for the 6 MV photon beam at a 15×15 cm^2 field size and 6 cm off-axis distance in the thick edge of wedged direction (x= 6 cm) would be 1.608 and 1.545 for 15^o and 60^o wedged photon beams

at a depth of 5 cm, respectively. To sum up, exit dose measurements, without applying the related $CF_{w,d}$, cause a major inaccuracy of nearly 10%. Therefore, determination of exit wedge correction factors at any off-axis position is important for estimating the absorbed dose value. Also, according to Huang et al., entrance dose evaluation, without applying the mentioned correction factors, would lead to an error rate of 9% [5].

The dose measurements using the ionization chamber, together with the exit surface diode measurements (Table 8), illustrate that the probable error in our proposed method was restricted to 1.5% for externally wedged photons, while the error rate would amount to 1.2% by applying diode measurements on the entrance surface [12]. Also, the error rate would be 0.5% by using a combination of entrance and exit surface measurements [13].

In a previous study, the accuracy of the model was reported up to 2% by estimating the absorbed dose at a desirable depth on the central beam axis and employing exit dose measurements [8]. Therefore, a strong correlation was evident between the absorbed dose calculations, using exit surface diode readings, and the measured dose values (as proposed in previous methods). Overall, the results of the present study showed that the estimated absorbed doseby the exit surface diode were true values, which could be compared with the prescribed doses at each depth of patient tissue.

5. Conclusion

Considering the difficulties in accurate positioning of diode s at central beam axis on the patient's exit surface, a larger tolerance range should be considered for wedged fields, while performing in vivo dosimetric evaluations. Evidently, evaluation of the dose delivered to a patient by using exit dose dosimeter for externally wedged beams is a reliable method for estimating the overall error

in the delivered dose at the end of radiation therapy.

Acknowledgments

The authors would like to thank the members of Radiotherapy Physics Department of Cancer Institute at Tehran University of Medical Sciences for their valuable assistance.

References

1. 1. Tung CJ. Wang HC, Lo HS , Wu JM , Wang CJ. In vivo dosimetry for external photon treatments of head and neck cancers by diodes and TLDs. Radiat Protect Dosim. 2004; 111(1):45-50.
2. 2. Rodriguez MI. Abrego E, Pineda A. Implementation of in vivo dosimetry with Isorad semiconductor diodes in radiotherapy treatment of the pelvis. Med Dosim. 2008; 33(1):14-21.
3. 3. Leuneus G, Dam JV, Durtex A, Schueren E. Quality assurance in radiotherapy by in vivo dosimetry . 2. Determination of the target absorbed dose. Radiother Oncol. 1990; 19(1):73-87.
4. 4. Rizzotti A, Compri C, Garusi F. Dose evaluation two patients irradiated by ^{60}CO beams , by means of direct measurement on the incident and on the exit surfaces. Radiother Oncol. 1985; 3(3):279-83.
5. 5. Huang K, Bice WS, Hidalgo – Salvatierra O. Characterization of an in vivo diode dosimetry system for clinical use. J Appl Clin Med Phys. 2003; 4(2):132-41.
6. 6. Loncol T, Greffe JL, Vynckeir S, Scalliet P. Entrance and exit dose measurements with semiconductors and thermoluminescent dosimeters: a comparison of methods and in vivo results. Radiother Oncol. 1996; 41(2):179-87.
7. 7. Essers M, Mijnheer BJ. In vivo dosimetry during photon beam radiotherapy. J Radiat Oncel Biol phys. 1999; 43(2):245-59.
8. 8. Millwater GJ, Macledo AS, Thwaites DI.In vivo semiconductor dosimetry as part of routine quality assurance.Br J Radiol. 1998; 71(6):661-8.
9. 9 Meijer GJ, Minken AWH , Ingen KM , Smulders B , Uiterwall H, Mijnheer B. Accurate in vivo dosimetry of a randomized trial of prostate cancer irradiation. Int J Radiat Oncol Biol phys. 2001; 49(5):1409-18.
10. 10. Heukelom S, Lanson JH, Mijnheer BJ. Comparison of entrance and exit dose measurements using ionization chambers and silicon diodes.Radiother Oncol. 1991; 36(1):47-59.
11. 11. Wolff T, Carter S, Langmack KA, Twyman NI , Dendy P. Characterization of a commercial n-type diode system . Br J Radiol. 1998; 71(11):1168-77.
12. 12. Mohammadkarim, Allahverdi M, Esfehani M, Nedaie H, Shirazi A, Geraily G. A method to improve the accuracy of diode in vivo dosimetry for external megavoltage photon beams filtered by wedges.Journal of Theoretical and Applied Physics.2013; 7:13:1-7.
13. 13. Allahverdi M, Mohammadkarim A, Esfehani M, Nedaie H, Shirazi A, Geraily G. Evaluation of off-axis wedge correction factor using diode dosimeters for estimation of delivered dose in external radiotherapy. J Med Phys. 2012; 37(4):32-9.
14. 14.Jornet N, Ribas M, Eudaldo T. In vivo dosimetry: Intercomparison between p-type based and n-type based diodes for the 16-25 MV energy range. Med Phys. 2000; 27(6):1287-93.
15. 15. Bisello F, Menichelli D, Scaringella M, Talamonti C, Zani M, Bucciolini M, Bruzzi M. Development of silicon monolithic arrays for dosimetry in external beam radiotherapy. Nucl Inst Meth in Phys Res A. 2015; 796:85-8.
16. 16. Oliveira FF, Amaral LL, Costa AM, Netto TG. In vivo dosimetry withsilicondiodesintotalbodyirradiation.Radiat Phys Chem. 2014; 95: 230-2.
17. 17. Edwards CR, Mountford PJ. Characteristics of in vivo radiotherapy dosimetry.Br J Radiol. 2009; 82(983):881-3.
18. 18. Tailor RC, Following DS, Hanson WF. A first order approximation of field size and depth dependence of wedge transmission. Med Phys. 1998; 25(5):241-4.
19. 19. Keall P, Zavgorodni S, Schmidt L, Hascard D. Improving wedged field dose distributions. Phys Med Biol. 1997; 42(11):2183-92.
20. 20. Mayler U, Szabo JJ. Dose calculation along the nonwedged direction for externally wedged beams: Improvement of dosimetric accuracy with comparatively moderate effort. Med Phys. 2002; 29(5):748-54.